Two New Binary Calcium−Aluminum Compounds: $Ca_{13}Al_{14}$, with a Novel Two-Dimensional Aluminum Network, and Ca_8Al_3, an Fe_3Al-Type Analogue[1]

Baoquan Huang and John D. Corbett*

Ames Laboratory—DOE and Department of Chemistry, Iowa State University, Ames, Iowa 50011

Received June 10, 1998

$Ca_{13}Al_{14}$ and Ca_8Al_3 are obtained by fusion of the appropriate mixture of the elements in Ta containers at 1100 °C followed by annealing at 600 °C or slow cooling, respectively. The structures of both compounds were determined by single-crystal X-ray means. $Ca_{13}Al_{14}$ crystallizes with monoclinic symmetry (space group $C2/m$ (no. 12), $Z = 2$, $a = 15.551(4)$ Å, $b = 9.873(2)$ Å, $c = 9.726(2)$ Å, $\beta = 108.09(2)°$), and Ca_8Al_3 has the triclinic Ca_8In_3-type structure ($P\bar{1}$ (no. 2), $Z = 2$, $a = 9.484(3)$ Å, $b = 9.592(3)$ Å, $c = 9.671(3)$ Å, $\alpha = 99.02(3)°$, $\beta = 101.13(3)°$, $\gamma = 119.55(3)°$). $Ca_{13}Al_{14}$ contains a two-dimensional Al network structure composed of planar hexagonal six-membered rings, planar rhombus (four-membered) rings, and trigonal three-membered rings. An electron count on the basis of the simple Zintl−Klemm formalism for three- and four-bonded Al in $Ca_{13}Al_{14}$ suggests the phase is closed shell. However, full band-structure calculations within the extended Hückel formalism indicate that it is metallic, with considerable Ca−Al covalency and, characterically, with all Al−Al bonding states just filled at E_F. The descriptor "metallic Zintl phase" is apt. Ca_8Al_3 contains isolated Ca and Al atoms and is slightly electron-rich relative to classical valence rules. Both compounds are good metallic conductors with Pauli-paramagnetic-like properties.

Introduction

The group 13 (IIIA) or triel elements show a remarkable variability in their formation of reduced homoatomic-bonded compounds. Boron has a unique chemistry, whereas, at the other extreme, elements of the gallium family (Ga, In, Tl) have in recent years been found to exhibit an extensive and remarkable variety of naked polyanions, mostly as alkali-metal compounds.[2,3] Structurally, these three elements exhibit both (a) networks of interbridged (or fused) triel clusters, sometimes rather complex, with a pronounced tendency to achieve, or come close to, valence (closed-shell and presumably semiconducting) compounds, especially for Ga, and (b) compounds containing isolated clusters that are likewise generally electron-precise and increase in frequency for the heavier In and Tl. Aluminum seems to have yet another chemistry. The marked distinction between Ga, In, Tl chemistry and that of Al must be brought about by the substantially altered, "unperiodic" trends associated with insertion of the three transition-metal series just ahead of the heavier three triels, making these smaller, softer, and more electronegative than usual.[4] Nowhere do these distinctions seem more evident than in the nature of the negative oxidation states of the triel elements in their compounds with more active metals. In fact, the compositions and structures for compounds of Al versus Ga with such metals show almost nothing in common.[5] For example, aluminum appears to form no compounds at all with Na−Cs. The sole exceptions appear to be for LiTr, Tr = Al, Ga, In, all of which exhibit a NaTl (stuffed diamond) structure,[6] and the isostructural Li_3Tr_2, Tr = Al, Ga.[6] Lithium is well-known for the exceptions it affords.[7]

More comparisons are possible among alkaline-earth-metal compounds of the triel metals. The intermetallic compounds that these form with aluminum are numerous, distinctive, and important in solid-state chemistry because they often have peculiar structural features and show unusual bonding and other physical properties. These examples also appear to exhibit clear features of covalent bonding in their crystal structures, although they are still inevitably metallic.[5] Although a variety of ternary and quaternary aluminum compounds have been extensively studied, some simple binary phase diagrams remain quite incomplete. The present article demonstrates that the binary Ca−Al system is one of the better examples of the latter. The current phase diagram dates to 1928, prior to general X-ray studies,[8] and only two compounds have been reported subsequently, $CaAl_4$ (tetragonal $BaAl_4$-type)[9] and $CaAl_2$ (cubic $MgCu_2$-type).[10] In 1992, Miller and Nesper[11] reported a study of the ternary Ca−Li−Al phase diagram and the discovery of a new pseudobinary $Ca_{8-x}Li_xAl_3$ with a calcium-poor equivalent of the Ca_8In_3 structure,[12] but they were not able to gain the pure Ca_8Al_3 binary.

(1) This research was supported by the Office of the Basic Energy Sciences, Materials Sciences Division, U.S. Department of Energy. The Ames Laboratory is operated by Iowa State University under Contract No. W-7405-Eng. 82.

(2) Belin, C.; Tillard-Charbonnel, M. *Prog. Solid State Chem.* **1993**, *22*, 59.
(3) Corbett, J. D. In *Chemistry, Structure and Bonding of Zintl Phases and Ions*; Kauzlarich, S. M., Ed.; VCH: New York, 1996; Chapter 3.
(4) Greenwood, N. N.; Earnshaw, A. *Chemistry of the Elements*, 2nd ed.; Butterworth-Heinemann: Woburn, MA, 1997; p 222.
(5) Miller, G. J. In *Chemistry, Structure and Bonding of Zintl Phases and Ions*; Kauzlarich, S. M., Ed.; VCH: New York, 1996; Chapter 1, p 44.
(6) Villars, P.; Calvert. L. D. *Pearson's Handbook of Crystallographic Data for Intermetallic Phases*, 2nd ed.; American Society for Metals International: Metals Park, OH, 1991.
(7) Nesper, R. *Prog. Solid State Chem.* **1990**, *20*, 1.
(8) *Binary Alloy Phase Diagrams*, 2nd ed.; Massalski, T. B., Ed.; American Society for Metals International: Materials Park, OH, 1990; Vol. 1, p 130.
(9) Nowotny, H.; Wormnes, E.; Mornhein, A. *Z. Metallkd.* **1940**, *32*, 39.
(10) Friauf, J. B. *J. Am. Chem. Soc.* **1927**, *49*, 3107.
(11) Miller, G. J.; Nesper, R. *J. Alloys Compd.* **1992**, *185*, 221.
(12) Fornasini, M. L. *Acta Crystallogr., Sect. C* **1987**, *43*, 613.

10.1021/ic980656h CCC: $15.00
Published on Web 10/07/1998

Our explorations of the possibilities that hydrogen or other light main-group nonmetals might stabilize alkali- or alkaline-earth-metal compounds with groups 13−15 elements[13−18] led to the discovery of the very unusual compound $Ca_{13}Al_{14}$. In addition, we found that the triclinic phase Ca_8Al_3 could also be formed in the absence of either hydrogen or lithium. In this paper, we present the syntheses, crystal structure determinations, and some bonding aspects and properties of the two compounds.

Experimental Section

Syntheses. The general techniques were previously described elsewhere.[14−17] The starting materials and their products were handled in a He- or N_2-filled gloveboxes that had a metered moisture level below 0.1 ppm (vol). The elements used were sublimed calcium (APL Engineered Materials, 99.99%) and aluminum (United Mineral and Chemical, 99.999%).

$Ca_{13}Al_{14}$. Single crystals of $Ca_{13}Al_{14}$ were initially obtained from reactions in the ternary Ca−Al−N system at 1100 °C followed by cooling at a rate of 20 °C h^{-1}. Once the composition was established by structural analysis, its high-yield synthesis was carried out by the following procedure. First, 3.0 g of Ca and Al with the nominal composition $Ca_{13}Al_{14}$ were arc-melted under Ar within a glovebox in order to avoid any side reaction between Al and the Ta container needed later. This product contained only ∼50% $Ca_{13}Al_{14}$ along with two secondary phases, $CaAl_2$ and Ca_8Al_3, according to its Guinier X-ray powder pattern. Next, the ingot was ground and welded under Ar into a Ta container, which was then jacketed by evacuated, flamed and sealed SiO_2 tubing to protect it from air. The contents were heated at 1100 °C, kept at that temperature for 4 h, and then slowly cooled at a rate of 10 °C h^{-1}. The yield of $Ca_{13}Al_{14}$ increased to ∼70%. Finally, the product was divided into three parts, which were similarly enclosed in Ta/SiO_2 and individually annealed at 900 °C for 5 days, 750 °C for 9 days, and 600 °C for 15 days, respectively, and quenched in water. The reactions at 900 and 750 °C showed decreased yields of the target phase, 20% and 30%, respectively, while the 600 °C process gave the desired product in a yield of ∼100%. (The yield was similar under vacuum conditions that would remove hydrogen.[17]) These reactions indicate that $Ca_{13}Al_{14}$ probably decomposes by a peritectic reaction between 600 and 750 °C. **Caution:** *Attempts to react the elements directly in a Nb container can be dangerous owing to the vigor of the AlBNb reaction!*

Ca_8Al_3. Single crystals of Ca_8Al_3 were initially obtained from a ternary Ca−Al−H system cooled from 1100 °C at a rate of 20 °C h^{-1}. It was later found that this phase could also be formed in the absence of hydrogen. The elements in an overall proportion Ca_8Al_3 (3 g total) were arc-melted under Ar, after which the Guinier pattern showed the yield of Ca_8Al_3 to be about 70%. The ingot was ground and welded in a Ta container under Ar, and this was in turn placed in fused silica tubing and connected to a vacuum source ($<10^{-5}$ Torr) in order to remove hydrogen. The contents were heated at 1100 °C, held there for 4 h, and cooled to room temperature at 10 °C h^{-1}, after which the sample was single-phase Ca_8Al_3 on the basis of X-ray powder diffraction.

Both phases have silvery appearances and are brittle and visibly stable in air for a few days. Guinier patterns were obtained from ground samples to which NIST silicon (a = 5.430 88 Å) had been added as an internal standard. These were mounted between pieces of cellophane tape, and the pattern was obtained with the aid of an Enraf-Nonius Guinier camera and Cu $K\alpha_1$ radiation. The Guinier films were measured with a computer-controlled microdensitometer, and the data were analyzed by the program SCAMPI to obtain peak positions relative to the Si standard lines. The X-ray patterns were indexed on the basis of the refined single-crystal models, and the lattice parameters were obtained by nonlinear least-squares means.

Structural Determinations. a. $Ca_{13}Al_{14}$. Several crystals were isolated and sealed into thin-walled capillaries, and Laue photographs were used to determine their singularity. Preliminary studies on a Rigaku AFC-6R rotating anode diffractometer (Mo Kα radiation, graphite monochromator) at room temperature established monoclinic symmetry, and the cell constants were determined from 25 centered reflections. A hemisphere of data was measured in an $\omega-2\theta$ scan mode for 2θ up to 56°. Three standard reflections were checked every 150 reflections during data collection, without observing any significant change. Assignment of the space group $C2/m$ (no. 12) was made on the basis of the systematic absences and a statistical analyses of intensity distribution, and this was supported by the subsequent successful refinement. The structure was solved by the direct methods via SHELXS-86[19] and refined on F_o by full-matrix least-squares methods with the aid of the TEXSAN package[20] on a VAX station. Preliminary refinements converged to $R(F)/R_w$ values of 3.6%/3.9%. Subsequently, absorption effects were corrected empirically according to ψ-scan curves for three strong reflections at different θ values and later, after isotropic refinement, by DIFABS,[21] which resulted in smaller and more uniform ellipsoids. After the first correction, 3537 reflections averaged to 1808 unique reflections (R_{int} = 8.7%, $I > 0$), and the final refinement with 918 observations and 72 variables converged with residuals $R(F)$ = 3.1%, R_w = 2.8%. (The final atomic positions were not significantly different from those before absorption corrections.) The largest residual peak and hole in the ΔF map were 0.55 $e^-/Å^3$ and −0.58 $e^-/Å^3$, respectively.

b. Ca_8Al_3. A few crystals were checked for singularity by Laue photographs, and diffraction data were collected from one at room temperature on a Rigaku AFC6R rotating anode diffractometer (Mo Kα radiation, graphite monochromator). For an assessment of the orientation matrix, 25 centered reflections located by a random search starting at $2\theta \approx 14°$ were used. In total, 3704 reflections were measured for the indicated triclinic cell in a hemisphere up to $2\theta = 56°$; of these, 2434 reflections were observed ($I/\sigma(I) > 3$). The structure was solved by direct methods via SHELXS-86. Preliminary anisotropic refinement with the TEXSAN package converged at the residuals $R(F)$ = 3.1%, R_w = 3.4%. Absorption effects were corrected empirically according to ψ-scan curves of three strong reflections at different θ values and later by DIFABS. Thermal parameters were smaller and more nearly spherical after the absorption corrections. The structure refinement involved 103 variables and converged at the residuals $R(F)$ = 2.8%, R_w = 2.9%. The largest residual peak and hole in the map were 0.40 $e^-/Å^3$ and −0.42 $e^-/Å^3$, respectively. Some data collection and refinement parameters for both phases are summarized in Table 1.

Physical Property Measurements. The electrical resistivities of both compounds were measured by the electrodeless high-frequency "Q" method.[17] A fractionated ground sample of each with an average particle diameter around 340 μm was separated and mixed with chromatographic Al_2O_3 in order to reduce contact between the sample particles. The mixture was loaded into a glass ampule and sealed under vacuum. The Q measurements were made at 35 MHz over 100 − 295 K, with readings every 10 K. Magnetic susceptibility data for both were measured at 3 T over 6 − 300 K on a Quantum Design MPMS SQUID magnetometer. A special fused silica container was used such that a 20−50 mg sample was held between the faces of two fixed silica rods.[22] The assembly was evacuated, backfilled with He, and sealed. Data were corrected for the diamagnetism of the container and the atom cores.

Band Calculations. Calculations by the extended Hückel tight-binding method[23] were done for $Ca_{13}Al_{14}$ with the aid of the QSAVEC package of programs developed by G. J. Miller at Iowa State. The

(13) Leon-Escamilla, E. A.; Corbett, J. D. *J. Alloys Compd.* **1994**, *206*, L15.
(14) Leon-Escamilla, E. A.; Corbett, J. D. *J. Alloys Compd.* **1998**, *265*, 104.
(15) Huang, B.; Corbett, J. D. *Inorg. Chem.* **1997**, *36*, 3730.
(16) Henning, R. W.; Leon-Escamilla, E. A.; Zhao, J.-T.; Corbett, J. D. *Inorg. Chem.* **1997**, *36*, 1282.
(17) Huang, B.; Corbett, J. D. *Inorg. Chem.* **1998**, *37*, 1892.
(18) Leon-Escamilla, E. A. Ph.D. Dissertation, Iowa State University, 1996.
(19) Sheldrick, G. M. *SHELXS-86*; Universität Göttingen: Germany, 1986.
(20) *TEXSAN*, version 6.0; Molecular Structure Corp.: The Woodlands, TX, 1990.
(21) Walker, N.; Stuart, D. *Acta Crystallogr.* **1983**, *A39*, 158.
(22) Guloy, A. M.; Corbett, J. D. *Inorg. Chem.* **1996**, *35*, 4669.
(23) Whangbo, M.-H.; Hoffmann, R. *J. Am. Chem. Soc.* **1978**, *100*, 6093.

Table 1. Some Crystallographic and Refinement Data

formula	$Ca_{13}Al_{14}$	Ca_8Al_3
fw	898.78	401.58
space group, Z	$C2/m$ (no. 12), 2	P (no. 2), 2
lattice dimen[a]		
a, Å	15.551(4)	9.484(3)
b, Å	9.873(2)	9.592(3)
c, D	9.726(2)	9.671(3)
α, deg	90	99.02(3)
β, deg	108.09(2)	101.13(3)
γ, deg	90	119.55(3)
V, Å^3	1419(1)	717(1)
d_{calc}, g cm^{-3}	2.103	1.859
μ, cm^{-1} (Mo Kα)	27.62	30.09
rel transm factors	0.89−1.00	0.74−1.00
R, R_w,[b] %	2.8, 2.9	3.1, 2.8

[a] Guinier data with Si as an internal standard, $\lambda = 1.540\,56$ Å, 23 °C. [b] $R = \sum||F_o| - |F_c||/\sum|F_o|$; $R_w = [\sum w(|F_o| - |F_c|)^2/\sum w(F_o)^2]^{1/2}$; $w = \sigma_F^{-2}$.

Table 2. Positional and Isotropic Temperature Factors (Å^2) for $Ca_{13}Al_{14}$

atom	x	y	z	B_{eq} (Å^2)[a]
Ca1	0.14628(7)	0.2027(1)	0.3659(1)	0.88(4)
Ca2	0.36159(7)	0.2819(1)	0.2275(1)	0.88(4)
Ca3	0.1969(1)	0	0.0851(2)	1.06(6)
Ca4	0.5036(1)	0	0.2024(2)	0.89(6)
Ca5	0	0	1/2	1.08(9)
Al1	0.1581(1)	0.3653(2)	0.0827(2)	0.90(6)
Al2	0.0013(2)	0	0.1578(3)	0.79(8)
Al3	0.2586(2)	0	0.6548(3)	0.86(8)
Al4	0.3398(2)	0	0.4311(3)	1.02(9)
Al5	0	0.3542(2)	1/2	0.84(8)
Al6	0	0.2249(2)	0	0.92(8)

[a] $B_{eq} = (8\pi^2/3)\sum'_i\sum'_j U_{ij} a_i^* a_j^* \vec{a}_i \vec{a}_j$.

orbital coefficients employed were those from Miller and Nesper,[12] while the H_{ii} parameters came from density functional theory calculations: Ca 4s, −6.56; 4p, −4.07; Al 3s, −11.79; 3p, −5.98 eV.[24] A 34 k-point mesh was used for calculations on the C-centered monoclinic structure.

Results and Discussion

Syntheses. Because $Ca_{13}Al_{14}$ apparently exhibits a peritectic melting behavior, the location of at least an approximate peritectic temperature is key to obtaining a pure sample. Rapid quenching from the melt followed by long annealing at various temperatures is required for this, and this procedure gave single-phase $Ca_{13}Al_{14}$ after 15 days at 600 °C but only mixtures at 750 and 900 °C. In other triel systems, this composition is evidently replaced by Sr_8Tr_7 phases for Tr = Al, Ga, and Ba_8Ga_7, all of which contain isolated Tr_4 tetrahedra and Tr_3 triangles.[25] Ca_8Al_3 may be congruently melting, or nearly so, since a single-phase product could be obtained by slow cooling of a fused mixture of the elements. Reactions run under high vacuum also gave these products in high yield, indicating the new compounds are not hydrides.

Structural Descriptions. Structures of $Ca_{13}Al_{14}$ and Ca_8Al_3 were refined from X-ray single-crystal diffraction data collected at room temperature. The final atomic coordinates, isotropic-equivalent displacement ellipsoids, and their estimated standard deviations are listed for both in Tables 2 and 3, respectively. Important distances are given in Tables 4 and 5. Refinement results for the structure of Ca_8Al_3 are very similar to those reported for $Ca_{8-x}Li_xAl_3$,[11] which is isotypic with Ca_8In_3[25] and contains isolated atoms. Our principal difference is that pure Ca_8Al_3 could not be obtained earlier, only the Li-substituted version. The structure details were described before, this structure being derived from the Fe_3Al (Li_3Bi) type by cation vacancies on tetrahedral sites.[11] Three cations, Ca5, Ca7, and Ca8, have only three Al neighbors (and hence a reduced potential), whereas the remainder have four (over 3.15−3.68 Å) in this rather distorted structure. The former group logically exhibits the largest B_{iso} values in the structure (Table 3), but all refine to about 100.9(2)% Ca occupancy. In the earlier work, reduced (90−94%) occupancies for only Ca7 and Ca8 were assigned a complementary lithium content. Although distances about these positions are not significantly larger in the present study, real effects from the presence of Li instead of Ca seem

Table 3. Atomic Positions and Isotropic Temperature Factors for Ca_8Al_3[a]

atom	x	y	z	B_{eq} (Å^2)
Ca1	0.4699(1)	0.2999(1)	0.34970(9)	1.33(2)
Ca2	−0.0802(1)	−0.2294(1)	0.89349(9)	1.29(2)
Ca3	0.1214(1)	−0.4021(1)	0.35079(9)	1.36(2)
Ca4	0.6666(1)	0.1211(1)	0.89067(9)	1.32(2)
Ca5	0.0423(1)	0.9392(1)	0.3308(1)	1.58(2)
Ca6	0.2988(1)	−0.4985(1)	0.89095(9)	1.35(2)
Ca7	0.2242(1)	−0.1530(1)	0.6996(1)	1.76(3)
Ca8	0.4527(1)	0.2866(1)	0.7010(1)	1.78(3)
Al1	0	1/2	0	1.16(5)
Al2	1/2	0	1/2	1.41(5)
Al3	0.8273(2)	0.6622(2)	0.4997(1)	1.32(3)
Al4	0.3241(2)	0.1593(2)	−0.0275(1)	1.23(3)

[a] Assignments are the same as in ref 11.

Table 4. Important Interatomic Distances and the Shortest Ca−Ca Contact (Å) in $Ca_{13}Al_{14}$

Ca1−Al1	3.242(2)	Al1−Ca3	3.436(2)
−Al2	3.217(2)	−Ca3	3.655(2)
−Al3	3.451(2)	−Ca4	3.261(2)
−Al3	3.320(2)	−Ca4	3.384(3)
−Al4	3.504(2)	Al2−Al2	3.057(5)
−Al4	3.506(2)	−Al6 (2×)	2.696(2)
−Al5	3.310(2)	−Ca1 (2×)	3.217(2)
−Al6	3.586(2)	−Ca2 (2×)	3.276(2)
Ca2−Al1	3.147(2)	−Ca3	3.249(3)
−Al1	3.276(2)	−Ca3	3.329(3)
−Al2	3.276(2)	−Ca5	3.335(3)
−Al3	3.282(2)	Al3−Al1 (2×)	2.812(3)
−Al4	3.493(2)	−Al4	2.834(4)
−Al5	3.150(2)	−Ca1 (2×)	3.320(2)
−Al6	3.534(1)	−Ca1 (2×)	3.451(3)
Ca3−Al1 (2×)	3.655(2)	−Ca2 (2×)	3.282(2)
−Al1 (2×)	3.436(2)	−Ca4	3.524(3)
−Al2	3.329(3)	−Ca5	3.832(3)
−Al2	3.249(3)	Al4−Al3	2.834(4)
−Al4	3.409(3)	−Al5 (2×)	2.774(3)
−Al6 (2×)	3.663(2)	−Ca1 (2×)	3.504(2)
Ca4−Al1 (2×)	3.261(2)	−Ca1 (2×)	3.506(2)
−Al1 (2×)	3.384(3)	−Ca2 (2×)	3.493(2)
−Al3	3.524(3)	−Ca3	3.409(3)
−Al4	3.867(3)	−Ca4	3.641(3)
−Al4	3.641(3)	−Ca4	3.867(3)
−Al5(2×)	3.249(2)	Al5−Al4 (2×)	2.774(3)
−Al6 (2×)	3.344(2)	−Al5	2.879(5)
Ca5−Al2 (2×)	3.335(3)	−Ca1 (2×)	3.310(2)
−Al3 (2×)	3.832(3)	−Ca2 (2×)	3.150(2)
−Al5 (2×)	3.497(3)	−Ca4 (2×)	3.249(2)
−Ca1	3.567(2)	−Ca5	3.497(3)
Al1−Al1	2.660(4)	Al6−Al1 (2×)	2.718(2)
−Al3	2.812(3)	−Al2 (2×)	2.696(2)
−Al6	2.718(2)	−Ca1 (2×)	3.586(2)
−Ca1	3.242(2)	−Ca2 (2×)	3.534(1)
−Ca2	3.147(2)	−Ca3 (2×)	3.663(2)
−Ca2	3.276(2)	−Ca4 (2×)	3.344(2)

(24) Vela, A.; Gázquez, J. L. *J. Phys. Chem.* **1988**, *92*, 5688.
(25) Fornasini, M. L. *Acta Crystallogr.* **1983**, *39C*, 943.

Table 5. Important Distances[a] and the Shortest Ca−Ca Contact (Å) in Ca_8Al_3

Ca1−Al2	3.526(1)	Al1−Ca2 (2×)	3.296(1)
−Al3	3.252(3)	−Ca3 (2×)	3.185(2)
−Al3	3.554(2)	−Ca4 (2×)	3.240(2)
−Al4	3.421(2)	−Ca6 (2×)	3.204(1)
Ca2−Al1	3.296(1)	Al2−Ca1 (2×)	3.526(1)
−Al3	3.595(2)	−Ca3 (2×)	3.528(3)
−Al4	3.614(3)	−Ca4 (2×)	3.554(2)
−Al4	3.146(2)	−Ca7 (2×)	3.431(2)
Ca3−Al1	3.185(2)	−Ca8 (2×)	3.379(1)
−Al2	3.528(3)	Al3−Ca1	3.252(3)
−Al3	3.633(2)	−Ca1	3.554(2)
−Al3	3.257(2)	−Ca2	3.595(2)
Ca4−Al1	3.240(2)	−Ca3	3.633(2)
−Al2	3.554(2)	−Ca3	3.257(2)
−Al4	3.659(2)	−Ca5	3.345(2)
−Al4	3.209(2)	−Ca5	3.380(2)
Ca5−Al3	3.345(2)	−Ca6	3.565(2)
−Al3	3.380(2)	−Ca7	3.253(2)
−Al4	3.679(2)	−Ca8	3.265(2)
Ca6−Al1	3.204(1)	Al4−Ca1	3.421(2)
−Al3	3.565(2)	−Ca2	3.614(3)
−Al4	3.601(2)	−Ca2	3.146(2)
−Al4	3.236(3)	−Ca4	3.659(2)
Ca7−Al2	3.431(2)	−Ca4	3.209(2)
−Al3	3.253(2)	−Ca5	3.679(2)
−Al4	3.255(2)	−Ca6	3.601(2)
Ca8−Al2	3.379(1)	−Ca6	3.236(3)
−Al3	3.265(2)	−Ca7	3.255(2)
−Al4	3.263(2)	−Ca8	3.263(2)
Ca1−Ca8	3.452(2)		

[a] Cutoff = 4.0 Å.

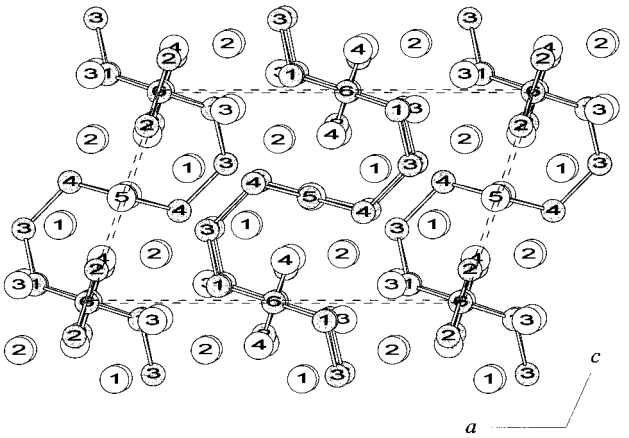

Figure 1. [010] view of the monoclinic cell of $Ca_{13}Al_{14}$ showing the two-dimensional rumpled Al layers edge-on (Ca, open; Al, gray).

evident in the refined atom positions in general, some of which differ from ours by over 50σ. The binary phase is one electron long to have a classical valence formulation, $(Ca^{2+})_8(Al^{-5})_3e^-$ (vec = $8^1/_3$).

$Ca_{13}Al_{14}$ crystallizes in a novel structure type with monoclinic symmetry (space group $C2/m$). The structure is made up of very unusual two-dimensional Al networks separated by Ca cations. A projection down [010] is shown in Figure 1. Note that the parallel Al sheets stacked along $\vec{a}$ are also separated by $b/2$, 4.94 Å, along this view direction. This makes the shortest intersheet distance between these, d(Al1−Al1) = 4.316 Å, beyond that of any significant direct interactions. The compound is too electron-rich to contain classical deltahedra (vec = 4.86 per atom); rather, Figure 2 shows how each puckered Al sheet is made up of six-, four- and three-membered rings. The planar six-membered rings consist of four Al1 and two Al6 atoms and have $2/m$ symmetry (Al6 atoms lie on sites of 2

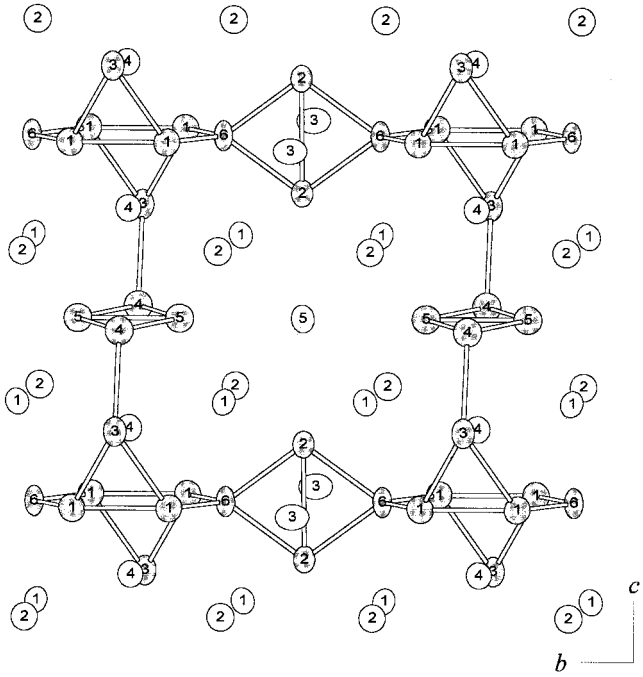

Figure 2. ~[100] view of a portion of a single aluminum layer constructed of six-, four-, and three-membered rings (Ca, open; Al, gray; ellipsoids at 99% probability level).

symmetry, while m symmetry bisects the Al1−Al1 bonds), thus resulting in two sets of equivalent bond distances: two Al1−Al1 (2.660(4) Å) and four Al1−Al6 (2.718(2) Å). The angles in the ring are 120.65(6)° (Al1−Al1−Al6) and 118.7(1)° (Al1−Al6−Al1) so that the isolated ring has close to hexagonal proportions.

There are two types of four-membered rings in this structure, both planar rhombuses. The first is generated by pairs of Al2 atoms that join two of the above six-membered rings at Al6 in an arrangement with $2/m$ symmetry (Al2 lies on m and Al6 on a 2-fold parallel to $\vec{b}$). This leads to four equal d(Al2−Al6) of 2.696(2) Å, while the Al2 pairs themselves have an apparently weak transannular interaction at 3.057(5) Å. The bond angles in the rhombus are 110.9(1)° and 69.1(1)° at Al2 and Al6, respectively, with 55.5° for Al6−Al2−Al2. A second rhombus formed by alternating Al4 and Al5 atoms has the same symmetry ($2/m$) and four slightly longer edges, d(Al4−Al5) = 2.774(3) Å, but a shorter d(Al5−Al5) = 2.879(5) Å than before and the corresponding angles of 117.5(1)°, 62.5(1)°, and 58.74(5)°. Both rhomboids may be described as pairs of condensed three-membered rings.

The result contains alternating six-membered rings and the first type of four-membered rings (with Al2) that lie perpendicular to each other and form infinite chains along $\vec{b}$. The six-membered rings are also cross-linked along $\vec{c}$ via Al3, and the second type of approximately parallel four-membered rings, Al4 plus Al5, giving infinite S-shaped chain sections of six-, three-, four-, and three-membered rings as shown in Figure 3. Each Al3 atom (on m) bonds to two Al1 atoms with equal distances (2.812(3) Å) to form a nearly trigonal ring (d(Al1−Al1) = 2.660(4) Å) and is bonded to one Al4 atom (Al3−Al4 = 2.834(4) Å) with a bond angle at Al3 of 120.5(1)°. Thus, the interchain linkages (Figure 1) generate puckered 20-atom rectangular rings built for four six-membered rings, four four-membered rings, and four three-membered rings plus two Al2 dimers. The combination of the linkages along b and c means that the chains shown in Figure 3 (and in the Table of Contents)

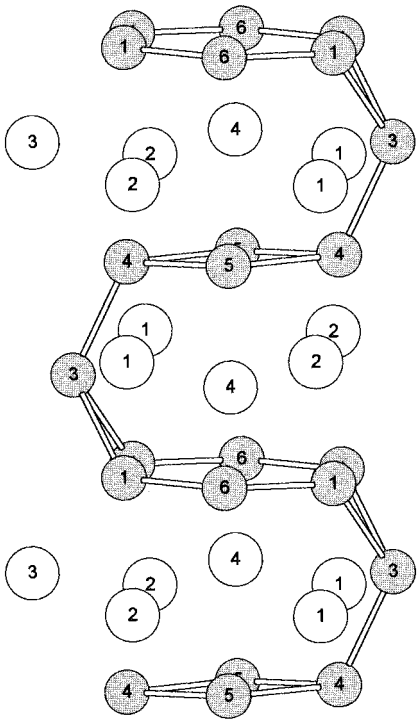

Figure 3. Section of the rumpled aluminum sheet in $Ca_{13}Al_{14}$ viewed along [010] (Ca, open; Al, gray; vertical).

represent only sections of rumpled 2D sheets, as are less clearly represented in Figure 1.

The polyhedra about each of the aluminum atoms are illustrated in Figure 4, while those about each calcium are given in the Supporting Information. The polyhedra in Figure 4 are oriented so as to make the shapes clear and not along any particular crystallographic direction. The six aluminum atoms are seven-, eight-, or nine-coordinate to calcium atoms in various, mainly irregular, polyhedra while the five calcium atoms have six, seven, eight, nine, or eleven aluminum neighbors. The Ca−Al distances in the low-symmetry $Ca_{13}Al_{14}$ fall in a range of 3.14−3.82 Å, compared with 3.33 Å in $CaAl_2$,[10] 3.35−3.52 Å in $CaAl_4$,[9] but 3.15−3.68 Å in Ca_8Al_3 (Table 5).

Properties. Molar magnetic susceptibility data for $Ca_{13}Al_{14}$ and Ca_8Al_3 at 3 T after core corrections are shown as a function of temperature in Figure 5. Both compounds show substantially temperature-independent values above about 50 K that are Pauli-paramagnetic in character, -6.5×10^{-4} emu/mol for $Ca_{13}Al_{14}$ and $\sim 1.5 \times 10^{-4}$ emu/mol for Ca_8Al_3. These are equivalent to 4.6 and 5.0 ($\times 10^{-5}$) emu/(mol Al), implying very similar densities of states (DOS) per Al. The absence of localized unpaired spins in the structures is as expected. Consistent with the magnetic properties, the temperature-dependent resistivity data indicate similar metallic behaviors, with $\rho_{296} \approx 55$ $\mu\Omega$·cm for $Ca_{13}Al_{14}$ and ~ 60 $\mu\Omega$·cm for Ca_8Al_3 at room temperature and $d\rho/dT$ for both of ~ 0.05 $\mu\Omega$·cm K^{-1}.

Bonding. The $Ca_{13}Al_{14}$ structure contains six independent Al atoms, with a multitude of Al−Al interactions over a 2.66−3.06 Å range (Pauling bond orders of 0.12−0.53 where $d_1 = 2.50$ Å[26]). The Al atoms divide into one tetrahedral four-bonded atom (4b-Al6), three three-bonded apical atoms (3b-Al1, -Al3, -Al4) and two planar three-bonded atoms, Al5 and Al2, all appropriate for a vec of 4.86 per Al atom. The compound can

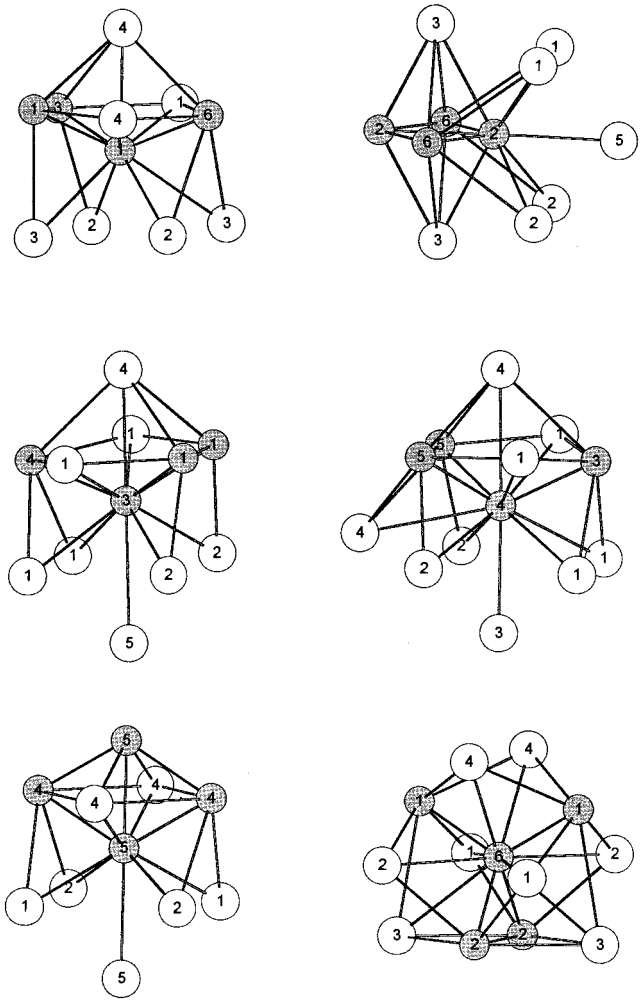

Figure 4. Environments around each of the aluminum atoms in $Ca_{13}Al_{14}$.

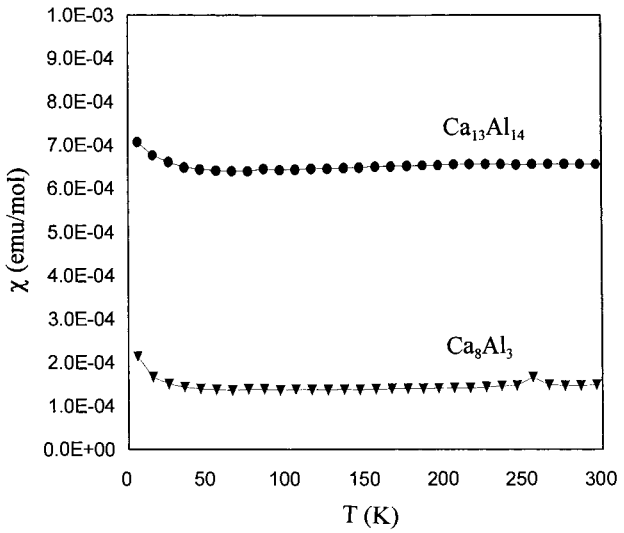

Figure 5. Molar magnetic susceptibilities (χ_M) of $Ca_{13}Al_{14}$ and Ca_8Al_3 at 3 T as a function of temperature.

accordingly be described with a closed-shell electron configuration, i.e., $(Ca^{2+})_{13}(4b\text{-}Al^{-})_2(3b\text{-}Al^{-2})_{12}$, according to simple Zintl−Klemm concepts if the electron transfer is that extreme and the unusual planar bonding at A12 and A15 can be (improbably) described as 3b-Al. This assignment is qualitatively helpful in understanding something about the stoichiom-

(26) Pauling, L. *The Nature of the Chemical Bond*, 3rd ed.; Cornell University Press: Ithaca, NY, 1960; p 400.

Table 6. Al−Al Bond Distances (Å) and Overlap Populations (OP) According to Calculations on the Isolated Layer in and on the Full Structure of $Ca_{13}Al_{14}$

bond	distance	substructure OP			full structure OP
		σ	π	sum	
Al1−Al1	2.660(4)	0.635	0.028	0.663	0.430
Al1−Al3	2.812(3)	0.501	0.006	0.507	0.3l8
Al1−Al6	2.718(2)	0.664	0.054	0.718	0.437
Al2−Al2	3.057(5)	0.187	−0.050	0.137	0.068
Al2−Al6	2.696(2)	0.588	0.018	0.606	0.346
Al3−Al4	2.834(4)	0.629	0.019	0.648	0.523
Al4−Al5	2.774(3)	0.511	0.020	0.53l	0.300
Al5−Al5	2.879(5)	0.337	−0.072	0.265	0.166

etry and structure of this compound, but it is certainly an oversimplification. Furthermore, it does not give us any hint as to why the Al−Al single bond lengths differ so much or as to whether the observed distances parallel either bond strengths or the more accessible overlap populations. (Matrix effects can often alter distances and give close contacts without the corresponding bonding electrons.[27,28])

Theoretical band structure calculations necessary to account for and explain some of the structural details in this compound were carried out on the two-dimensional Al network substructure (i.e., without Ca atoms) as well as on the complete three-dimensional structure, according to the EHTB approximation. Some Al−Al distance and bond population data from both approaches are given in Table 6, principally to emphasize in a pedagogical way how much the electrons assigned in the Mulliken approximation either to bonds (overlap populations) or to the atoms (not listed) in the Al layer calculation are delocalized back onto the calcium atoms when the calcium is included. This is not surprising for atoms with such relatively large fields and small electronegativity difference ($\Delta\chi = 0.61$ according to Pauling, 0.07 for Mulliken[29]).

The left side of Figure 6 shows the total DOS obtained from band calculations on the Al layer (top) and the total $Ca_{13}Al_{14}$ structure (bottom), with the calcium contributions also projected out in the latter. Clearly, the solid is expected to be metallic, as observed. The full band structure along high-symmetry lines in the region around the Fermi level reveals that E_F clearly cuts through several bands, particularly along the $\Gamma \rightarrow Y \rightarrow Z \rightarrow \Gamma$ directions. Inspection of the orbital coefficients at Γ for the first eight bands below E_F shows marked antibonding π^* contributions in four from Al2−Al2 and, especially, A15−A15 interactions, some close to E_F. These are easily discerned in the COOP data (overlap populations as a function of E) shown in Figure 7 for the planar atom pairs A15−A15 (left) and A12−A12 (right), where values to the left of the center line in each are negative (antibonding). (Such effects are well-known characteristics of planar arrays and lead in general to gapless solids.) Examinations of other COOP curves or of other calcium atom projections in the DOS show there are no particularly localized or distinctive contributions for other atoms. Figure 6 (lower left) illustrates how well the Ca DOS follow the Al contributions.

These calculations also afford distinctive atom populations, and these are compared with the number of neighbors of both kinds and the average d(Al−Al) and d(Al−Ca) in Table 7. Of course, Al6 is unique because it alone is four-bonded to other

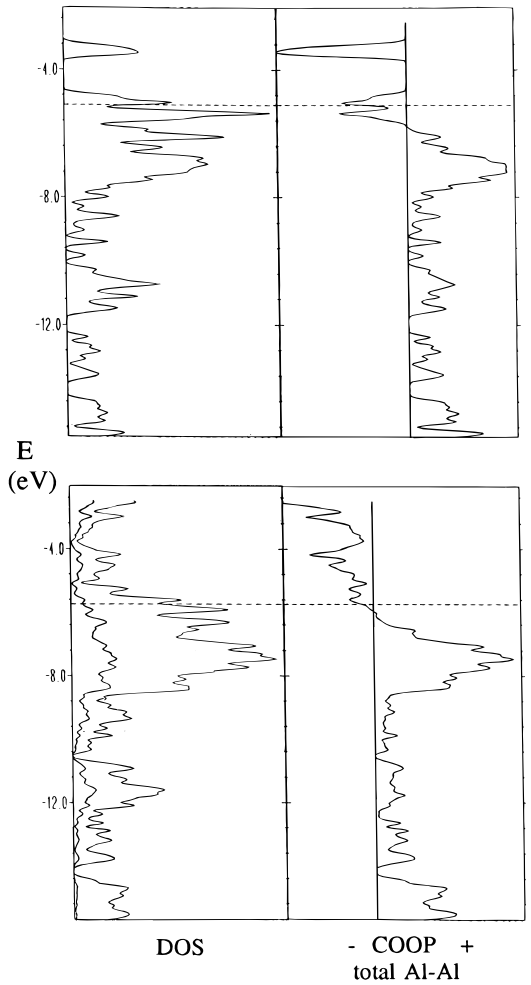

Figure 6. Densities of states from extended Hückel calculations on (top) the Al layer and (bottom) the complete structure of $Ca_{13}Al_{14}$ with Ca contributions projected out. The dashed line marks E_F. The right sides are the corresponding COOP curves for total Al−Al bonding.

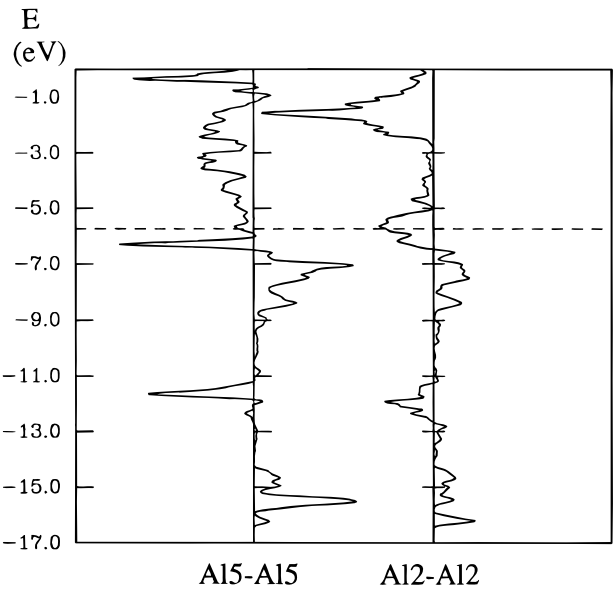

Figure 7. Portion of the COOP curves for the relatively weak Al5−Al5 and Al2−Al2 interactions in $Ca_{13}Al_{14}$(s).

Al and thereby exhibits longer (Al−Ca) values. On the other hand, the most exposed 3b- (or 2b-) Al2 and Al5 atoms have the shortest (Al−Ca) values for seven neighbors, the smallest overlap population sums to other bonded Al, and the highest

(27) Corbett, J. D. *J. Solid State Chem.* **1981**, *37*, 335.
(28) Maggard, P. A.; Corbett, J. D. *Inorg. Chem.* **1998**, *37*, 8l4.
(29) Shriver, D. F.; Atkins, P.; Langford, C. H. *Inorganic Chemistry*, 2nd ed.; W. H. Freeman: New York, 1994; p 44.

Table 7. Aluminum Atom and Bond Populations and Distance Averages (Å) for $Ca_{13}Al_{14}$

Al atom	Al atom popl	rank (highest = 1)	no. Al neighbors	$\bar{d}$(Al−Al)	ΣAl−Al OP	no. Ca neighbors	$\bar{d}$(Al−Ca)	rank (shortest = 1)
1	3.73	2	3	2.730	1.56	7	3.343	2
2	4.04	1	3 (2[a])	2.816 (2.696[a])	0.94 (0.82[a])	7	3.271	1
3	3.77	2	3	2.819	1.55	8 (7[b])	3.433 (3.376[b])	3 (2)
4	3.79	2	3	2.794	1.45	9 (8[b])	3.547 (3.507[b])	4
5	3.99	1	3	2.809	0.99	7	3.274	1
6	3.39	3	4	2.707	1.96	8	3.532	4

[a] Omitting the long transannular distance, 3.057 Å. [b] Omitting one long $\bar{d}$(Al−Ca) > 3.8 Å. The next longer distances are ≤3.66 Å.

atom populations. The Al−Al distances in this network thus turn out to be rather poor predictors of relative overlap populations.

A more striking and informative effect is seen in the lower right in Figure 6, the COOP curve for *all* Al−Al bonding in the solid. The total Al−Al overlap populations in the solid change from clearly bonding to antibonding very close to E_F; in other words the compound's structure serves to maximize Al−Al bonding. Clearly, the Al−Al structure does matter, and the phase can be aptly and reasonably described as a "metallic Zintl phase".[3,7]

This last observation is in fact rather general. Nesper[7,30] and Miller[5,11] have both discussed the enticing structures of and bonding in a number of these generally nonclassical triel compounds, Li_2Ga, $CaAl_4$, $CaAl_2$, $CaGa_2$, $Ca_3Al_2Si_2$, $LaAl_3$, $TmAl_3$, $CaLi_xAl_{2-x}$, Ba_4Al_5, $Li_xCa_{8-x}Al_3$, and so forth. All have complex structures with extensive aluminum atom sublattices, strongly implicating the presence of electron localization in Al−Al bonds, although the bonding details in some are very complex and unclear. Nonetheless, all are metallic and many exhibit the characteristic shown in the lower right of Figure 6, that the total Tr−Tr overlap populations are positive just up to E_F.

Clearly, aluminum provides many novel and sometimes puzzling results in the structure and bonding of compounds with the more active metals, being virtually unique in comparison with other triel elements B, Ga, In, Tl. The structure motifs are generally unusual, and that for $Ca_{13}Al_{14}$ is seemingly unprecedented. One can imagine that more surprises will turn up on thorough searches of this and other alkaline-earth-metal−aluminum or ternary systems, possibly when hydride interference[13,14] is carefully avoided.

Acknowledgment. The authors thank Jerome Ostenson for the magnetic measurements and Gordon J. Miller for advice on and the use of his program package.

Supporting Information Available: Three tables with further data collection and refinement information and anisotropic displacement parameters and an illustration of the environment around the Ca atoms in $Ca_{13}Al_{14}$ (4 pages). Ordering information is given on any current masthead page.

IC980656H

(30) Nesper, R. *Angew. Chem., Int. Ed. Engl.* **1991**, *30*, 789.